Investigation on two-phase flow instability in steam generator of integrated nuclear reactor*

Jing Jian-Gang (荆建刚) and Chen Ting-Kuan (陈听宽)
(Xi'an Jiaotong University, Xi'an 710049)

Abstract In the pressure range of 3~18 MPa, high pressure steam-water two-phase flow density wave instability in vertical upward parallel pipes with inner diameter of 12 mm is studied experimentally. The oscillation curves of two-phase flow instability and the effects of several parameters on the oscillation threshold of the system are obtained. Based on the small perturbation linearization method and the stability principles of automatic control system, a mathematical model is developed to predict the characteristics of density wave instability threshold. The predictions of the model are in good agreement with the experimental results.
Keywords Integrated nuclear reactor, Steam generator, Two phase instability, Density wave oscillation

1 Introduction

In recent years, developing integrated nuclear power reactor is considered more and more necessary in many countries. In this kind of reactor, the reactor core, steam generator and other auxiliary equipment are designed as a whole and put together into the pressure shell. The reactor has the advantages of simple structure, light weight, convenient start and adjustment, good safety properties and so on. It is especially used as naval ship power, heat supply, sea water desalinization and other industrial powers and has a brilliant perspective.

Steam generator is the key equipment of the integrated nuclear power reator, which transmits the heat produced in the core to the water of secondary side. Whether it is running safely is related to the work of the whole reactor. It is known that the secondary side's pressure of the steam generator is generally lower than 7 MPa, therefore there exists serious two-phase flow hydraulic instability. Under unreasonable design circumstances, two-phase flow instability may cause flow excursion or oscillations of flow rate and thermal parameters. Sustained flow oscillations may cause mechanical vibration of components or disturb system control. It can also affect the critical heat flux, leading boiling crisis and wall temperature leap. The persistence of such flow oscillation could eventually lead to tube failure due to thermal fatigue. So, two-phase flow instability is the key problem in developing integrated nuclear reactor.

Density wave oscillation is the most common type of two-phase flow instabilities. Despite extensive studies had been made during the last three decades on the subject of density wave instability, the researches of two-phase flow instability mostly focused on one vertical or horizontal tube, and were done with boiling freon[1,2]. Under high pressure and temperature conditions, the researches of two-phase flow instability in parallel pipes with water as working fluid are much less. In the present study, density wave oscillation in parallel pipes under practical working conditions is studied experimentally and theoretically, and the effect of system parameters such as mass velocity, pressure, inlet subcooling, etc. on the instability threshold is analysed. The results of this paper can be used for the design of steam generator in integrated nuclear reactor to prevent from the occurrence of density wave instability.

2 Apparatus and experiments

2.1 Test apparatus

The high pressure water experimental loop is shown schematically in Fig.1. The demineralized water from water tank is pumped by high pressure pump, then divided into two lines — the test section line and the by-pass one for regulating the water flow rate. Water of the test section system enters preheater through

*The Project Supported by National Natural Science Foundation of China
Manuscript received date: 1995-11-20

orifice flowmeter, where it is heated up to the desired temperature. Water flowing out of the preheater flows into the test section through (or not) a surge tank, where it is heated to boiling. After the test section, the steam-water two-phase mixture flows into the condenser, finally returns back to the water tank.

The test section consists of two parallel 1Cr18Ni9Ti stainless steel pipes with inner diameter of 12 mm. Its whole length is 7.31 m, the heated section of which is 4.2 m. The two parallel pipes are linked by the upper and bottom header with the distance between two pipes of 0.8 m.

The test section is heated by large electrical current produced by transformers passing through the pipes themselves. In this experiment, the preheater is heated by 3 large electrical current transformers with the maximum power of 380 kW. Each tube of the test section is heated seperately with the maximum power of 180 kW. The test section and preheater both are insulated by aluminum silicate ceramics material.

Three Venturi flowmeters are installed respectively at the entrance of the test section and at that of each tube. At the entrance and exit, 2 NiCr-NiSi jacked thermocouples of Φ3 mm are installed to measure the fluid temperature. The test section pressure drop, inlet pressure, exit pressure and the pressure drop of each tube are measured with 1151 HP capacitive pressure drop transducer and DBY-140 pressure transducer. The 80 NiCr-NiSi thermocouples with Φ0.5 mm are attached to the outer surface of each tube to measure wall temperature profile along circumferential and axial direction. All signals from transducers go into MS-1215 high speed data acquisition system and IMP3595C serial data acquisition unit as well. These data acquisition systems are connected to IBM computer for data monitoring, storing and processing. In addition, continuous oscillation curves are recorded by a function recorder.

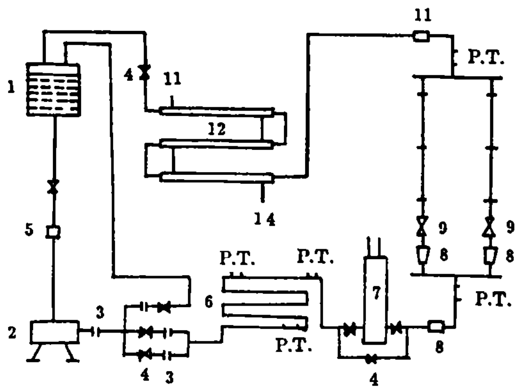

Fig.1 Schematic diagram of high pressure water loop

1. water tank, 2. high pressure pump, 3. orifice, 4. valve 5. filter 6. preheater 7. surge tank 8. inlet venturi 9. inlet valve 10. test section 11. exit venturi 12. condenser 13. inlet of cooling water 14. exit of cooling water, T. thermocouples P. pressure

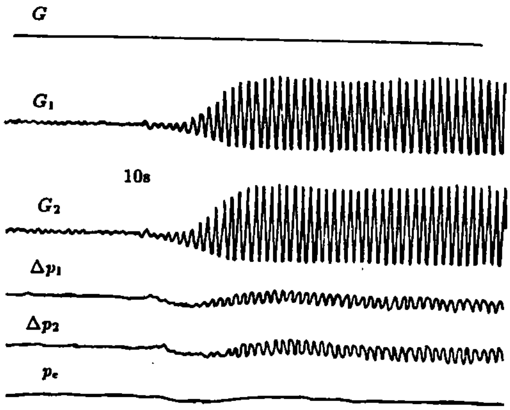

Fig.2 Recordings of typical density wave oscillation in parallel tubes

$p_e = 10\,\mathrm{MPa}$, $G=1000\,\mathrm{kg/(m^2{\cdot}s)}$, $\Delta t_{sub} = 30°\mathrm{C}$

2.2 Experimental procedure

a. Select a working condition, the parameters of which such as pressure, flow rate, inlet subcooling and inlet resistance coefficient are fixed.

b. Increase the preheater electrical power in order to improve the fluid's temperature up to the selected inlet subcooling of the test section.

c. After a stabilizing time, increase the electrical power of the test section by a small step.

d. Record the relevant data when the system is steady.

e. Continue steps c and d till the sustained oscillations are observed, then record the average data and instability data. The above procedure is then repeated for different working conditions to cover the allowable range.

2.3 Experimental results

For conditions closing to saturated vapor state at the exit of the test section (positive slope region on the hydraulic power curve), density wave oscillations are observed. Fig.2 shows recordings of the total flow rate and the flow rate of each tube, pressure drop of each tube and the exit pressure under the typical density wave oscillation. As it can be seen from the figure, the whole flow rate and exit pressure do not oscillate; the flow rate of the two tubes oscillates with an exactly contrary phase. The phenomena can be explained as follows: according to the mechanisms of two-phase flow instabilities, the absorbing and releasing of energy appears accompanying with the oscillations. When there is no compressible volume for energy exchange at upstream of the test section, then the two parallel tubes are taken as compressible volumes from each other for energy exhange. Therefore, the oscillations with an exactly contrary phase are observed.

The following are the experimental results of the effects of system parameters on the density wave oscillation.

The effect of the system pressure. With the increase in the system pressure, the oscillation's threshold heat flux q_{jx} and threshold exit quality x_{jx} increase, so does the system's stability (Fig.3). When the system pressure goes up to 1 MPa, there is no density wave oscillation. The period of oscillations becomes larger with the system pressure increasing (Fig.4).

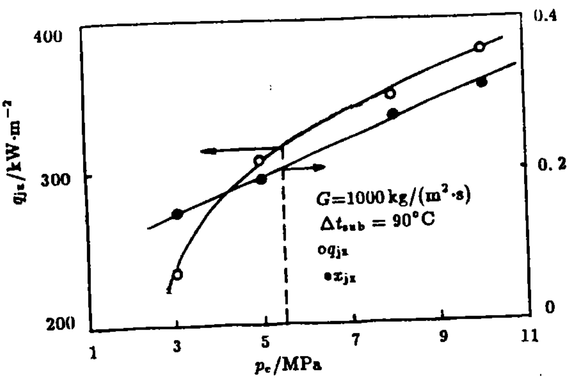

Fig.3 The effect of system pressure

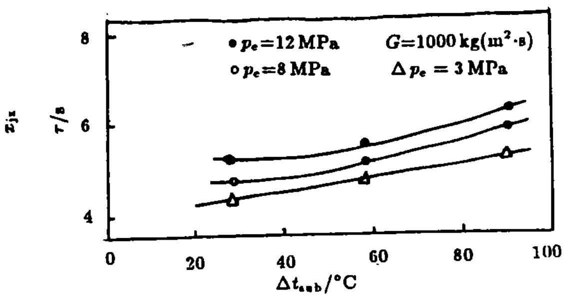

Fig.4 The effects of pressure and inlet subcooling on oscillation period (τ)

The effect of the mass velocity. With the mass velocity increasing, the threshold heat flux always increases, so does the system's stability. And the oscillation's period becomes shorter, but the amplitude larger.

The influence of the inlet subcooling. The inlet subcooling increases, so do the threshold heat flux and the system's stability. And the oscillation period always becomes longer (Fig.4).

The influence of the inlet resistance coefficient. With the inlet resistance coefficient of each tube increasing, the threshold heat flux and quality always increase, so does the system's stability.

The influence of unsymmetrical heat flux. Fig.5 shows the experimental result of threshold heat flux q_{jx} versus the heat flux ratio of two parallel tubes. With the unsymmetrical heat flux ratio decreasing, the threshold heat flux increases, so does the system's stability.

For simplicity, meanings of all symbols used in this paper are listed as follows:

D= inner diameter, g= acceleration speed of gravity, h= enthalpy, H= heated length, N_{OR}= inlet resistance coefficient, p= pressure, Δp= pressure drop, Q= volume heat flux, q= aera heat flux, R= hydraulic resistance, s=

complex variable, t= time, Δt_{sub}= inlet subcooling, V= specific volume, v= flow velocity, G= mass velocity, $\bar{x}$= average mass fraction, z= length coordinate, β= void fraction, δ= small perturbation, ρ= density, x= mass fraction; for subscripts, B=boiling, e=exit, ex=external loop, f=liquid, fg = difference between two phases, g = vapor, i = inlet, jx = boundary, SF = single phase, TP = two phase, 0 = steady state, sat = saturated.

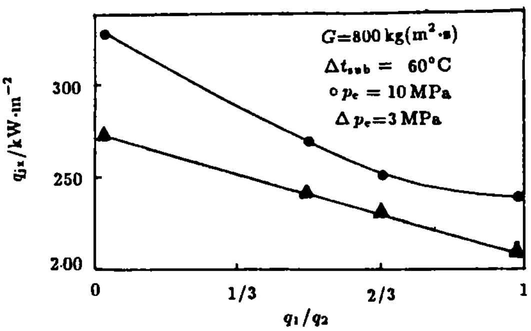

Fig.5 The influence of unsymmetrical heat flux

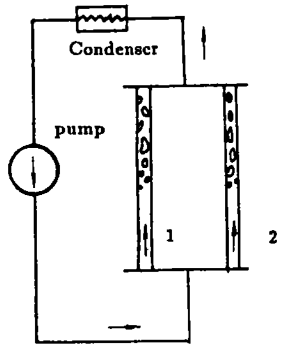

Fig.6 Simplified diagram of the system

3 Mathematical formulation

The practical test system may be simplified as Fig.6. First, consider the flow condition of one tube and assume: one-dimensional flow, thermal equilibrium between two phases, uniform heat flux. By use of the variable density model of two-phase flow, the conservation equations can be expressed as:

For two phase flow region

$$\frac{\partial}{\partial t}[\rho_f(1-\beta)+\rho_g\beta]+\frac{\partial}{\partial z}[\rho_f v_f(1-\beta)+\rho_g v_g\beta]=0 \quad (1)$$

$$\frac{\partial}{\partial t}[\rho_f h_f(1-\beta)+\rho_g h_g\beta]+\frac{\partial}{\partial z}[\rho_f v_f h_f(1-\beta)+\rho_g v_g h_g\beta]=Q \quad (2)$$

$$\begin{aligned}\frac{\partial}{\partial t}[\rho_f v_f(1-\beta)+\rho_g v_g\beta]+\frac{\partial}{\partial z}[\rho_f v_f^2(1-\beta)+\rho_g v_g^2\beta]= \\ -\frac{\partial p}{\partial z}-[\rho_f(1-\beta)+\rho_g\beta]g-(\frac{\partial p_f}{\partial z})_{TP}\end{aligned} \quad (3)$$

$$v_g=\gamma v_f \quad (4)$$

Let $\beta=0$, the conservation equation in single-phase region can be obtained.

Boundary conditions are as follows:

At inlet:

$$G(0,t)=G_i(t);\ h(0,t)=h_i(t) \quad (5)$$

At boiling boundary z_B:

$$\begin{aligned}h(z_B,t)=h_{sat};\ \beta(z_B,t)=0; \\ G(z_B,t)=G_i(t)\end{aligned} \quad (6)$$

Slip ratio γ could be expressed as:

$$\gamma=\frac{1-\beta}{k_1-\beta} \quad (7)$$

$$k_1=0.71+1.45\times10^{-8}p \quad (8)$$

Single phase frictional pressure drop gradient $(\frac{\partial p_f}{\partial z})_{SF}$ and resistance coefficient λ are calculated according to Ref.[3].

Two-phase frictional pressure drop gradient $(\frac{\partial p_f}{\partial z})_{TP}$ is given by

$$(\frac{\partial p_f}{\partial z})_{TP}=\Phi\cdot(\frac{\partial p_f}{\partial z})_{SF} \quad (9)$$

Two-phase frictional coefficient Φ are calculated according to Ref.[4].

Variables and their reference variables (RV) are listed in Table 1.

Table 1 Variables and its reference variables

Variable	RV	Variable	RV
z, z_B	H	Q	Q_0
t	H/v_{i0}	v_f, v_g	v_{i0}
G, G_i	$\rho_f v_{i0}$	p	$\rho_f v_{i0}^2$
ρ	ρ_f	$h-h_{sat}$	$h_{fg}/(\rho_f V_{fg})$

Then make the conservation equations and boundary conditions of two-phase region and single phase region dimensionless. For convenient writing, the dimensionless variables are expressed by the symbols of their variables and the following dimensionless numbers are introduced:

$$N_Q = \frac{V_{fg} H Q_0}{h_{fg} v_{i0}} \tag{10}$$

$$N_S = \frac{\rho_f V_{fg}}{h_{fg}} \Delta h_{sub} \tag{11}$$

$$N_F = \frac{v_{i0}^2}{gH} \tag{12}$$

$$N_R = \frac{\lambda_0 H \Phi_0}{2D} \tag{13}$$

$$F_1 = \frac{1-\beta+\beta\gamma}{1-\beta+\eta\beta\gamma} \tag{14}$$

$$F_2 = \frac{1-\beta+\eta\beta\gamma^2}{(1-\beta+\eta\beta\gamma)^2} \tag{15}$$

$$\eta = \rho_g/\rho_f \tag{16}$$

Dimensionless equations and boundary conditions are as follows:

Two-phase region:

$$\frac{\partial \rho}{\partial t} + \frac{\partial G}{\partial z} = 0 \tag{17}$$

$$\frac{\partial}{\partial z}(F_1 \cdot G) = N_Q \cdot Q \tag{18}$$

$$\begin{aligned} &\frac{\partial G}{\partial t} + \frac{\partial}{\partial z}(F_2 \cdot G^2) = \\ &-\frac{\partial p}{\partial z} - \frac{1}{N_F}\rho - N_R G^{1.75}\Phi \end{aligned} \tag{19}$$

Single phase region:

$$\frac{\partial G}{\partial z} = 0 \tag{20}$$

$$\frac{\partial h}{\partial t} + G\frac{\partial h}{\partial z} = N_Q \cdot Q \tag{21}$$

$$\begin{aligned} &\frac{\partial G}{\partial t} + \frac{\partial G^2}{\partial z} = \\ &-\frac{\partial p}{\partial z} - \frac{1}{N_F} - N_R G^{1.75} \end{aligned} \tag{22}$$

At inlet:

$$G(0,t) = G_i(t); h(0,t) = -N_S \tag{23}$$

At boiling boundary:

$$\begin{aligned} h(z_B,t) = 0; \rho(z_B,t) = 1; \\ G(z_B,t) = G_i \end{aligned} \tag{24}$$

4 Solution of conservations

4.1 Solution of the continuity and energy equations

Single-phase region:

Linearize Eqs.(20,21) by small perturbation, then do Laplace transformation to them, one obtains,

$$\delta G(z,s) = \delta G_i \tag{25}$$

$$\delta h(z,s) = N_Q \int_0^z e^{-s(z-z')} dz' \cdot (\delta Q - \delta G_i) + \delta h_i(s) e^{-sz} \tag{26}$$

Two-phase region:

Let Eq.(18) integrated, small-perturbed and linearized and $U_0 = -\frac{1}{F_1} \cdot \frac{dF_1}{d\rho}$, one obtains,

$$\delta G = U_0 \delta\rho + \frac{1}{F_1}[(F_1 - 1)\delta Q - N_Q \delta z_B + \delta G_i] \tag{27}$$

Combine Eq.(27) and Eq.(17), let $\delta\rho_m = U_0\delta\rho$, $\alpha = \frac{1}{F_1}$, $z_m = \int_0^z \frac{dz}{U_0}$, $\delta e = \delta G_i - \delta Q - N_Q \delta z_B$, one obtains,

$$\frac{\partial \delta\rho_m}{\partial t} + \frac{\partial \delta\rho_m}{\partial z_m} = -\frac{d\alpha}{dz_m}\delta e \tag{28}$$

Do Laplace transformation to Eq.(28), then solve it, obtain,

$$\delta\rho_m(z_m,s)=\int_{z_{Bm}}^{z_m} e^{S(z'_m-z_m)}\cdot(-\frac{\mathrm{d}\alpha}{\mathrm{d}z'_m})\mathrm{d}z'_m\delta_{\mathrm{e}}+\delta\rho_m(z_{\mathrm{B0}},s)e^{-s(z_m-z_{Bm})} \tag{29}$$

At steady boiling boundary z_{B0}, Eq.(24) is small perturbed, we obtain by reorganization,

$$\delta\rho_m(z_{\mathrm{B0}},s)=-\delta h_{\mathrm{B}}(s) \tag{30}$$

$$\delta G(z_{\mathrm{B0}},s)=\delta G_{\mathrm{i}}(s) \tag{31}$$

$$\delta h_{\mathrm{B}}(s)=-N_Q\delta z_{\mathrm{B}} \tag{32}$$

Therefore, the solutions of the continuity and energy equations are as follows:
Two-phase region:

$$\delta\rho_m(z_m,s)=\int_{z_{Bm}}^{z_m} e^{s(z'_m-z_m)}\cdot(-\frac{\mathrm{d}\alpha}{\mathrm{d}z'_m})\mathrm{d}z'_m\delta_{\mathrm{e}}-\delta h_{\mathrm{B}}(s)e^{s(z_{Bm}-z_m)} \tag{33}$$

$$\delta G(z,s)=\delta\rho_m+\delta Q+\alpha_0\delta_{\mathrm{e}} \tag{34}$$

Single-phase region:

$$\delta\rho_m=0;\qquad \delta G=\delta G_{\mathrm{i}} \tag{35}$$

$$\delta_{\mathrm{e}}=\delta G_{\mathrm{i}}-\delta Q+\delta h_{\mathrm{B}} \tag{36}$$

$$\delta h_{\mathrm{B}}(s)=-\int_0^{z_B} N_Q e^{s(z'-z_B)}\mathrm{d}z'(\delta G_i-\delta Q)+\delta h_i(s)e^{-sz_B} \tag{37}$$

The relations of the above perturbation variables are expressed in Fig.7. Define the following transfer functions,

$$G_1=\frac{\partial G}{\partial G_i}=(1+H_3)(H_1+\alpha_0)+H_2H_3 \tag{38}$$

$$G_2=\frac{\partial\rho_m}{\partial G_{\mathrm{i}}}=(1+H_3)H_1+H_2H_3 \tag{39}$$

$$G_3=\frac{\partial z_{\mathrm{B}}}{\partial G_{\mathrm{i}}}=-\frac{H_3}{N_Q} \tag{40}$$

4.2 Solution of momentum equations

Two-phase region:

Integrate Eq.(19), we obtain,

$$\begin{aligned}-\Delta p_{\mathrm{TP}}&=\int_{z_{\mathrm{B}}}^1\frac{\partial G}{\partial t}\mathrm{d}z+(F_2G^2)\big|_{z_{\mathrm{B}}}^1\\&+\frac{1}{N_F}\int_{z_{\mathrm{B}}}^1\rho\mathrm{d}z+N_{\mathrm{R}}\int_{z_{\mathrm{B}}}^1 G^{1.75}\Phi\mathrm{d}z\end{aligned} \tag{41}$$

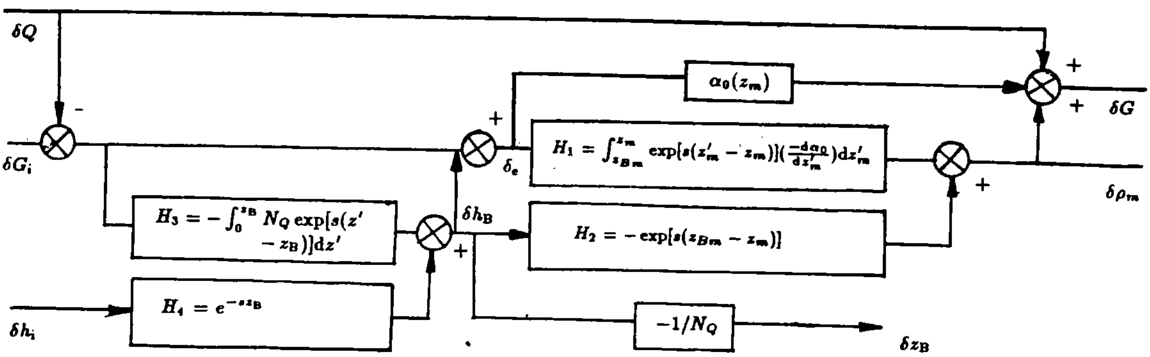

Fig.7 Transfer relations of small perturbation variables

Let Eq.(43) small-perturbed, linearized and Laplace-transformed and $R_{\mathrm{TP}} = -\frac{\delta\Delta p_{\mathrm{TP}}}{\delta G_{\mathrm{i}}}$, obtain,

$$\begin{aligned} R_{\mathrm{TP}} = {} & s\int_{z_B}^{1} G_1 \mathrm{d}z + (\tfrac{\mathrm{d}F_2}{\mathrm{d}\rho} G_2(z=1) \\ & +2F_2G_1(z=1) - 2 + \tfrac{1}{N_F}\int_{z_B}^{1} G_2 \mathrm{d}z \\ & +N_B\int_{z_B}^{1}[1.75 + \tfrac{1}{\Phi_0}(\tfrac{\mathrm{d}\Phi}{\mathrm{d}G})_0\Phi_0 G_1 \mathrm{d}z \\ & +N_R(1-\Phi_0)G_3 \end{aligned} \tag{42}$$

Single-phase region:

Deal with Eq.(22) in the same way as mentioned above, obtain,

$$R_{\mathrm{SF}} = -\frac{\delta\Delta p_{\mathrm{SF}}}{\delta G_{\mathrm{i}}} = s z_{\mathrm{B}} + 1.75 N_R z_{\mathrm{B}} + N_{\mathrm{OR}} \tag{43}$$

The hydraulic resistance for the whole tube is expressed as

$$R = R_{\mathrm{TP}} + R_{\mathrm{SF}} \tag{44}$$

4.3 Characteristic equation of parallel tubes

According to the electrical current law of closed circuit, for the system expressed by Fig.6. We obtain:

$$R_{\mathrm{ex}} + \frac{1}{1/R_1 + 1/R_2} = 0 \tag{45}$$

As mentioned above, when density wave oscillation appears in parallel tubes, the total flow rate is kept constant, the flow rates of two tubes oscillate with an exactly contrary phase. Therefore, the hydraulic resistance R_{ex} of external loop equals ∞. Eq.(45) could be simplified as

$$R_1 + R_2 = 0 \tag{46}$$

This is the characteristic equation of parallel tubes. In order to stabilize the system, all the roots of the characteristic equation must lie on the left side of the complex plane[5]. The stability of the system can be also estimated by Nyquist stability criterion, examining whether the Nyquist cure encircles point (–1, i0). In the present study, Nyquist criterion is used to decide the stability of system.

5 Results and discussion

Fig.8 illustrates the experimental and predicted threshold heat flux under two working conditions. As it can be seen from the figure, both results are in good agreement.

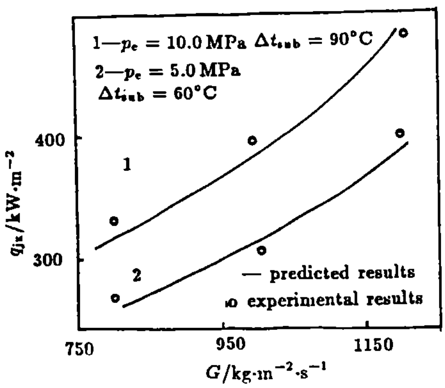

Fig.8 Comparison between predicted results and experimental results

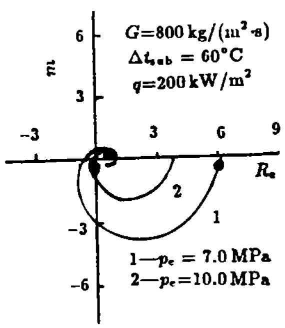

Fig.9 The effect of system pressure

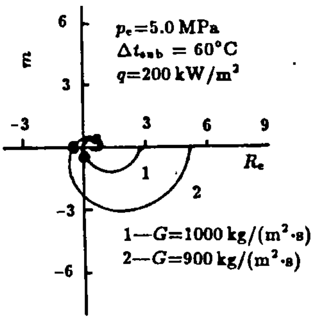

Fig.10 Effect of mass velocity

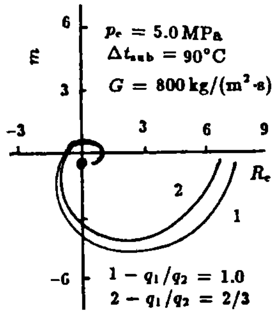

Fig.11 The effect of unsymmetrical heat flux

Figs.9,10,11 illustrate the effects of pressure, mass velocity and unsymmetrical heat flux on the stability threshold, respectively. As it can be seen from the figures, with the increase in pressure, mass velocity and unsymmetrical heat flux, the distance between point $(-1, i0)$ and the intersection point of Nyquist curve with real axis becomes larger, so the system's stability is improved. This results coincide with the experimental results as mentioned above.

6 Conclusions

a. Density wave oscillations are observed in the positive slope region on the hydraulic power curve. Its period is shorter, from 4 to 20 s.

b. Under the conditions of no compressible volume at the upstream of the test section, when density wave oscillations appear, the total flow rate and the exit pressure are kept constant, the flow rates of two parallel tubes oscillate with an exactly contrary phase.

c. With the increases in pressure, inlet resistance coefficient, inlet subcooling and mass velocity, the threshold heat flux is improved, so is the system's stability.

d. With the increases in pressure and inlet subcooling, the oscillation period becomes longer; with the increases in mass velocity and heat flux, the period becomes shorter.

e. Unsymmetrical heat flux improves the stability of the system.

f. Density wave oscillation could be prevented by improving system pressure, inlet resistance coefficient of each tube, mass velocity and controlling the inlet subcooling suitably.

g. The mathematical model is in satisfactory agreement with the experimental results. It can be used as reference for the stability design of steam generator in integrated nuclear power reactor.

References

1 Fukuda K, Kato A, Hasegawa S. Two-phase flow instability at low flow rate conditions, J Nucl Sci and Technol, 1984; 21(7):491~500

2 Yokomizo O. Nucl Eng and Des, 1986; 92:141~151

3 Sumida I, Kawai T. J Nucl Sci and Technol, 1978; 15:323~337

4 Lin Zonghu. Gas-liquid two-phase flow in pipelines and their applications in engineering (in Chinese). Xi'an Jiaotong University Press, 1993; 28~29

5 Taleyarkhan R P, Podowski M Z, Lahey R T Jr. Nucl Eng and Des, 1986; 93:39~50